

Development of a photoactivatable fluorescent protein from *Aequorea victoria* GFP

George H. Patterson, Jennifer Lippincott-Schwartz

Cell Biology and Metabolism Branch, National Institute of Child Health and Human Development,
National Institutes of Health, Bethesda, MD 20892

ABSTRACT

Photoactivation, the rapid conversion of photoactivatable molecules to a fluorescent state by intense irradiation, can be used to mark and monitor selected molecules within cells¹. We report a photoactivatable variant of the *Aequorea victoria* green fluorescent protein (GFP) based on a mutation at position 203 that upon intense irradiation with 413 nm light exhibits a stable 60-100 fluorescence increase under 488 nm excitation. The photoactivated form of this mutant named photoactivatable GFP (PA-GFP), is stable under a number of conditions. PA-GFP can be used to analyze protein dynamics in living cells, offering enormous potential for addressing outstanding questions in protein trafficking and turnover, organelle dynamics, and cell lineage patterns.

Keywords: Photoactivation, fluorescence imaging, T203, green fluorescent protein

Correspondence should be addressed to J. L.-S. (e-mail: lippincj@mail.nih.gov)

1. INTRODUCTION

Techniques to monitor protein dynamics within cells are extremely important for the characterization of numerous regulatory processes that involve protein turnover, diffusion, binding/dissociation or translocation. Over the past ten years, the *Aequorea victoria* green fluorescent protein (GFP) has provided an invaluable research tool for studying these processes in cell and developmental biology^{2,3}. Fusion of GFP with a protein-of-interest produces a genetically-encoded and specific tag that can be expressed and monitored in living cells without additional secondary labels. This property plus GFP's remarkable stability under various environmental extremes⁴⁻⁷ and its numerous spectra altering mutations³ has led to its preeminence as an imaging tool in cell and developmental biology.

Methods associated with monitoring the behavior of fluorescently-tagged proteins within cells have been reviewed extensively⁸⁻¹⁴. Generally, these methods rely on the irradiation-induced destruction (photobleaching) of the chromophores of fluorescently-labeled proteins located in selected regions-of-interest. Photobleaching is a useful approach because it perturbs the steady-state distribution of fluorescence within the cell by indirectly highlighting a population of molecules. The highlighted molecules in this case are the ones located outside the photobleached region. By monitoring their movement into the photobleached region, insight into their compartment access, binding constants, and diffusional mobility can be gained.

In contrast to photobleaching, photoactivation directly highlights a population of molecules and is usually associated with the photo-induced uncaging of an inert caged compound to produce an active molecule¹. In fluorophore uncaging experiments, the molecules have little or no fluorescence prior to photoactivation and display greatly increased fluorescence output after release of the caging group. While photoactivation of caged fluorescent molecules has been

used for many years to highlight directly cells and proteins, fluorescent proteins that display photo-induced increases in fluorescence (photoactivation) have been less common¹⁴.

One of the first examples of GFP photoactivation took advantage of the photoconversion that takes place in the chromophore of wild type GFP. Initially reported for *Aequorea victoria* wtGFP by Chalfie and colleagues², the photoconversion phenomenon¹⁵ leads to a decrease in the major absorbance peak (~400 nm) and an increase in the minor absorbance peak (~475 nm). By imaging using 488 nm and briefly irradiating with 365 nm laser light, Yokoe and Meyer were able to selectively enhance wild type GFP fluorescence and thereby monitor diffusion in living cells¹⁶. A second approach relied on the phenomenon that several mutants of the *Aequorea victoria* GFP photoconvert into a red fluorescent species under low oxygen conditions and intense 488 nm irradiation^{17,18}. Such phenomenon has been used to monitor protein diffusion in bacteria, but is inappropriate for eukaryotic systems due to the requirements for anaerobic conditions. A third method of photoactivation is based on the red fluorescence from a protein isolated from *Anemonia sulcata*, asFP595 (asCP). Such fluorescence was enhanced by pre-irradiation with green light, but the activated signal had a half-life of ~10 seconds¹⁹. A recent improvement on asCP is the A148G mutant called KFP1. It gives a stable 30-fold increase in red fluorescence after photoactivation²⁰. A fourth photoactivation method uses the DsRed protein from *Discosoma*. It relies on photobleaching the protein's red fluorescence to unmask its green fluorescence²¹. The basis for this is that the DsRed protein requires several hours to mature from the green into the red fluorescent species and it self-associates to form tetramers. Therefore, some complexes contain both green and red emitting species. Selective photobleaching of the red species disrupts resonance energy transfer from the green species and this leads to an increase in the green fluorescence. A final photoactivation method utilizes the Kaede protein, isolated from *Trachyphyllia geoffroyi*, which displays a remarkable red-shift in both excitation and emission upon photoactivation. This results in a remarkable 2000-fold increase in red-to-green fluorescence²².

2. METHODS

2.1 Plasmid constructs.

Plasmid constructions and site-directed mutagenesis is described elsewhere²³.

2.2 Protein expression and purification.

All pRSET plasmids were transformed into Epicurian Coli BL21 (DE3) pLysS (Stratagene, La Jolla, CA). The proteins were expressed, purified, and prepared as previously described^{23,24}.

2.3 Spectroscopy.

A Beckman DU 640 UV-Visible Spectrophotometer was used to perform absorbance measurements on GFPs in phosphate buffered saline (PBS) pH 7.4. Fluorescence excitation and emission measurements were performed on a SPEX 1681 Fluoromax-3 spectrofluorometer with a 150-W xenon arc lamp (Jobin Yvon, Inc., Edison, NJ). Fluorescence excitation spectra were acquired by scanning 1 nm intervals from 350 nm to 525 nm collecting the fluorescence emission using 25 nm slit widths centered at 550 nm.

2.4 Cell culture.

COS 7 cells were grown in Dulbecco's Modified Eagle Media (DMEM) containing 10% fetal bovine serum (FBS), 2 mM glutamine, 100 U/ml penicillin, and 100 mcg/ml streptomycin. Cells grown in Lab-Tek chambers with #1.0 borosilicate cover glasses (Nalge Nunc International, Naperville, IL) or on #1.5 round cover glasses (A. Daigger & Company, Wheeling, IL) were transfected for 24-48 h using FuGENE 6 transfection reagent (Roche, Indianapolis, IN). Live cell experiments were performed in DMEM as above without phenol red and containing 25 mM HEPES pH 7.5.

2.5 Microscopy.

Photoactivatable GFP imaging was performed in multi-tracking mode on a Zeiss LSM510 laser scanning confocal microscope (Carl Zeiss, Thornwood, NY) with a 63X Plan Apochromat 1.4 NA objective and a 413/488 dichroic mirror. One track was used to image pre-activated proteins under excitation using 488 nm line of a argon ion laser (Lasos, Germany). Photoactivation was performed with high level of 413 nm Enterprise II krypton ion laser (Coherent, Auburn, CA). Emission was collected with a 505 nm long-pass filter.

3. RESULTS AND DISCUSSION

3.1 PA-GFP development

Here, we discuss the discovery and testing of a photoactivatable fluorescent protein from the *Aequorea victoria* GFP²³. GFP consists of an eleven strand β -barrel surrounding an α -helix that contains the chromophore^{25,26}. In wild type GFP, the cyclization of amino acids S65, Y66, and G67 forms the chromophore²⁷, which normally exists as a mixed population of neutral phenols and anionic phenolates producing the major 397 nm and minor 475 nm absorbance peaks, respectively^{28,29}. Upon intense illumination of the major peak, the chromophore is thought to undergo a proton transfer and photoconvert into the anionic form via an intermediate^{3,15,30}. Rotation of T203 during irradiation³¹ positions the threonine hydroxyl group where it is thought to stabilize the anionic chromophore^{28,29}.

The shift in the chromophore population to the anionic form increases absorbance at the minor excitation wavelength, which, in turn, leads to \sim 3-fold increase in fluorescence upon excitation at 488 nm¹⁶. An example of the spectral shift is shown in figure 1 using a purified sample of WEGFP (wild type-like enhanced GFP)²³ that has been irradiated for increasing time periods with 413 nm laser light. The non-photoactivated protein (Fig. 1; open circles) has the major \sim 400 nm peak and minor \sim 475 nm peak. After only 5 minutes of 413 nm irradiation (Fig. 1; open squares), a decrease in the \sim 400 nm peak and increase in the \sim 475 nm peak is observed. This phenomenon is continued over

longer irradiation times until the chromophore population is shifted entirely or photobleached. Significant absorbance at 488 nm prior to photoconversion (Fig. 1; open circles) results in moderate fluorescence background and subsequently results in modest signal enhancement. To improve upon the WEGFP photoactivation properties¹⁶, we generated mutant GFPs with decreased absorbance at 488 nm to increase the contrast between the pre-photoactivation and post-photoactivation fluorescence signal. A previously described T203I mutant of GFP^{32,33} reduced the minor peak absorbance while the major absorbance peak at \sim 400 nm was retained. We began by testing the photoactivation properties of this mutant and found that upon irradiation with 413 nm laser light, 488 nm excited fluorescence increased by \sim 16-fold. The accepted model for wild-type GFP photoconversion suggested that the anionic chromophore was stabilized by the hydroxyl group of T203^{28,29}, the results with the T203I mutant indicated that this hydroxyl group was not necessary for production of a stable photoactivated protein. Therefore, we substituted T203 with every other amino acid and determined the spectral and photoactivation characteristics of these mutants. The wide range of effects these mutations had on both the absorbance spectra and the photoactivation are indicated in figure 2.

The alanine (T203A), cysteine (T203C), glutamic acid (T203E), glycine (T203G), histidine (T203H)³⁴, isoleucine (T203I)³²⁻³⁴, lysine (T203K), leucine (T203L), methionine (T203M), asparagine (T203N), glutamine (T203Q), serine (T203S), valine (T203V)³⁴, and tryptophan (T203W) substitutions decreased the minor peak absorbance and maintained a major peak at \sim 400 nm (Fig. 2; closed circles). Both the tyrosine (T203Y)³⁴ and phenylalanine (T203F)³⁴ mutations had peaks at \sim 400 nm, but both had red-shifted minor peaks of similar or greater absorbance compared with WEGFP (T203)²³. For undetermined reasons, three substitutions, aspartic acid (T203D), proline (T203P), and arginine (T203R), produced proteins with little or no absorbance in the 400 nm or 475 nm regions (data not shown). Strikingly, upon photoactivation of the other 17 variants in a cuvette with 413 nm laser light, all but the T203E, T203F, T203K, T203M, and T203W displayed noticeable increases in their minor peak absorbance (Fig. 2 open squares). The T203F and T203Y mutants had spectra with increased absorbance in the 475-500 nm region, which suggested an increased population of anionic chromophore prior to photoactivation. On the other hand, T203E and T203W

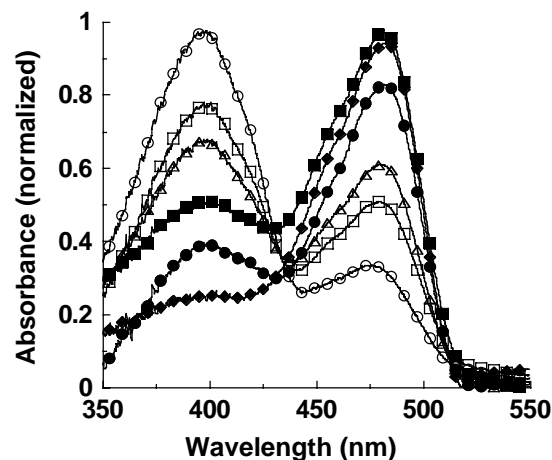


Figure 1. Photo-induced conversion of WEGFP absorbance spectrum. Purified, His-tagged WEGFP was placed in a quartz cuvette and irradiated with 25 mW of 413 nm laser light at room temperature. Absorbance spectra were acquired at 0 minutes (open circles), 5 minutes (open squares), 10 minutes (open triangles), 20 minutes (closed squares), 30 minutes (closed circles), and 60 minutes (closed diamonds). These data are normalized to the absorbance at 400 nm for the pre-photoactivated sample (time 0).

mutations maintained ~400 nm peaks even after photoactivation, suggesting the neutral chromophore was stabilized. However, T203W was not fluorescent whereas T203E retained green fluorescence emission (data not shown). Interestingly, the T203K and T203M had decreases in their ~400 nm peak upon photoactivation²³ but maintained their minor peaks after irradiation (Fig. 2; open squares).

The spectral changes associated with substitutions are of interest, but our goal was to produce a protein capable of

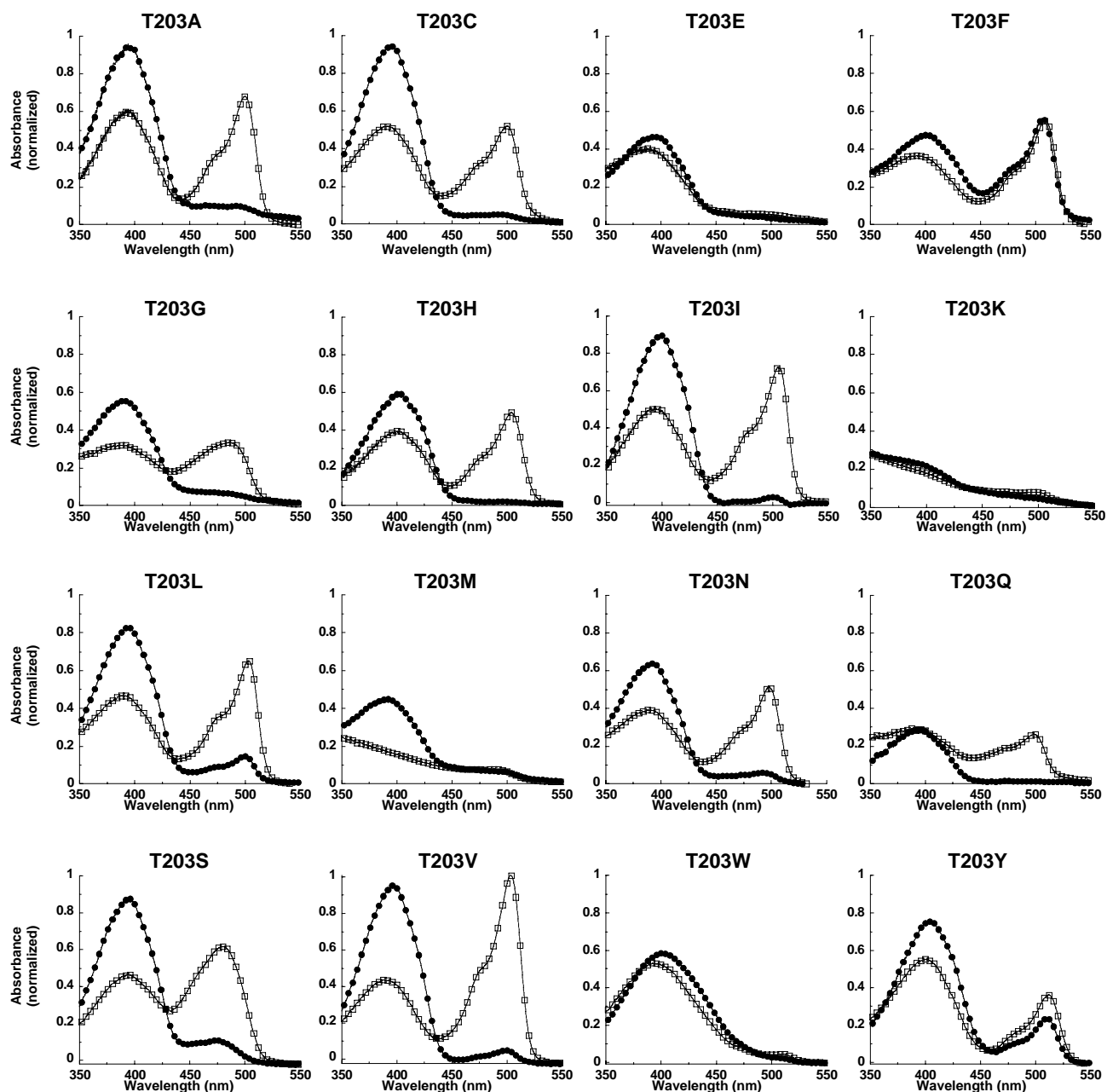


Figure 2. Absorbance spectra of pre-photoactivated and post-photoactivated T203 mutants. Absorbance spectra were acquired on purified, His-tagged proteins with the indicated substitutions at the threonine 203 position before (closed circles) and after (open squares) irradiation with 25 mW of 413 nm laser light for 30 minutes at room temperature. Spectra are normalized to the absorbance at 280 nm.

increased contrast between pre- and post-photoactivation fluorescence images. Therefore, we next determined the fold activation for WEGFP and many of the T203 mutant GFPs under imaging conditions. For these experiments, purified preparations of proteins were distributed within 15% polyacrylamide gels to produce a homogeneous and immobile population of protein. While monitoring the fluorescence under 488 nm excitation, the embedded proteins were irradiated with 413 nm laser light. The fold increases in fluorescence qualitatively correlated with the spectral changes in figure 2. Interesting exceptions were the T203K and T203M which showed little increase in their minor absorbance

peak but displayed moderate photoactivation (9.5 and 17-fold, respectively) of its 488 nm excited fluorescence under imaging conditions²³. Our screen of the possibly useful T203 mutants revealed fluorescence increases upon photoactivation ranging from 2.9-fold for the WEGFP to 101-fold for the T203H mutant²³. This exceptional mutant was renamed PA-GFP and further characterized for use as an imaging tool.

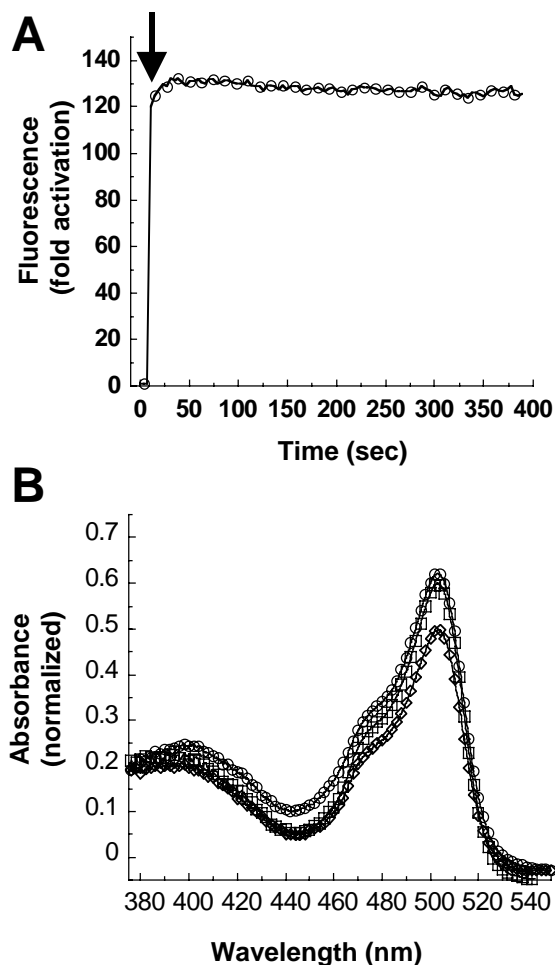


Figure 3. Stability of the photoactivated state of PA-GFP. (A) Purified, His tagged PA-GFP was embedded in polyacrylamide for imaging using 488 nm excitation. This graph represents the quantification of the fluorescence increase upon photoactivation and subsequent imaging. The arrow indicates the time point of photoactivation. The data are normalized to the initial time point before photoactivation. (B) Purified, His tagged PA-GFP was irradiated with 40 mW of 413 nm laser light for 30 minutes at room temperature. Absorbance spectra were acquired immediately after photoactivation (day 0; open circles), three days after photoactivation (day 3; open squares), and seven days after photoactivation (day 7; open diamonds). Spectra are normalized to the absorbance at 280 nm.

3.2 PA-GFP stability

As with any fluorophore, the stability of PA-GFP fluorescence can be a limiting factor in an imaging experiment. Because PA-GFP undergoes such a dramatic spectral alteration, it was possible that it could rapidly revert to its pre-activated state, which would limit or negate its usefulness as an imaging tool. To investigate this possibility, we examined the stability of the photoactivated PA-GFP. One test for this is shown in figure 3A, in which purified PA-GFP embedded in polyacrylamide was photoactivated and continuously imaged over 400 seconds. For this example, the fold-activation was ~120-fold. Furthermore, quantification over the course of the experiment suggested that once PA-GFP is photoactivated, the photoactivated state does not rapidly revert to the pre-activated state and nor does it rapidly photobleach. Indeed, the photostability of photoactivated PA-GFP compared reasonably well with EGFP in photobleaching studies²³. The stability of the photoactivated PA-GFP was further tested by monitoring the absorbance spectra over a 7 day period (Fig. 3B). After photoactivation of purified PA-GFP on day 0 (Fig. 3B; open circles), the protein was incubated at 37°C for 7 days while monitoring its absorbance spectrum. The day 3 spectrum (Fig. 3B; open squares) compared well with that on day 0 with little change in either the ~400 nm or ~504 nm peak. Both peaks were slightly decreased on day 7 (Fig. 3B; open diamonds). Importantly, the ratio of the ~504 nm and ~400 nm peaks remained constant over the experiment, demonstrating that the photoactivated PA-GFP does not revert to its pre-activated state even after 1 week.

We examined the stability of the different states of PA-GFP in more detail by performing denaturing and refolding experiments on non-photoactivated (pre-activated) and photoactivated (post-activated) PA-GFP. For these experiments, proteins were (1) maintained in a non-denatured state by dilution with phosphate buffered saline (PBS) pH 7.4, (2) denatured by dilution with 8M urea and maintained

in the denatured state, or (3) refolded by dilution in PBS before acquiring of fluorescence excitation spectra. Figure 4A shows excitation spectra of pre-activated PA-GFP. The non-denatured PA-GFP (Fig. 4A; open circles) had a peak at ~400 nm with little fluorescence produced in the 488 nm region, while the denatured PA-GFP (Fig. 4A; open squares) showed little fluorescence across the spectrum. Importantly, upon refolding by dilution with PBS (Fig. 4A; open diamonds), a peak at ~400 nm was recovered and the protein still had little fluorescence in the 488 nm region. Similar experiments performed on post-activated PA-GFP are shown in figure 4B. The non-denatured post-activated PA-GFP (Fig. 4B; open circles) had a minor fluorescence excitation peak at ~400 nm and a major peak located at ~504 nm. Denatured post-activated PA-GFP (Fig. 4B; open squares) had little fluorescence excitation in either wavelength range, whereas upon refolding (Fig. 4B; open diamonds), PA-GFP displayed peaks at both ~400 nm and ~504 nm, similar to the non-denatured post-activated protein. Figure 4C represents an experiment in which non-photoactivated PA-GFP

was diluted in PBS to maintain the non-denatured state or denatured with 8M urea. These samples were then subjected to photoactivation with 413 nm laser light as the samples in figures 1 and 2. The non-denatured protein was diluted again in PBS, while the denatured protein was diluted with 8M urea to maintain the denatured state or refolded by dilution with PBS. The non-denatured protein (Fig. 4C; open circles) expectedly displayed excitation peaks at ~400 nm and ~504 nm, while the denatured protein (Fig. 4C; open squares) displayed little fluorescence excitation in either region. On the other hand, the denatured protein which was irradiated with 413 nm laser light refolded into the pre-activated state (Fig. 4C; open diamonds). These data indicate that upon refolding, PA-GFP reacquires the state it had prior to denaturation and that photoactivation is dependent on properly folded molecules.

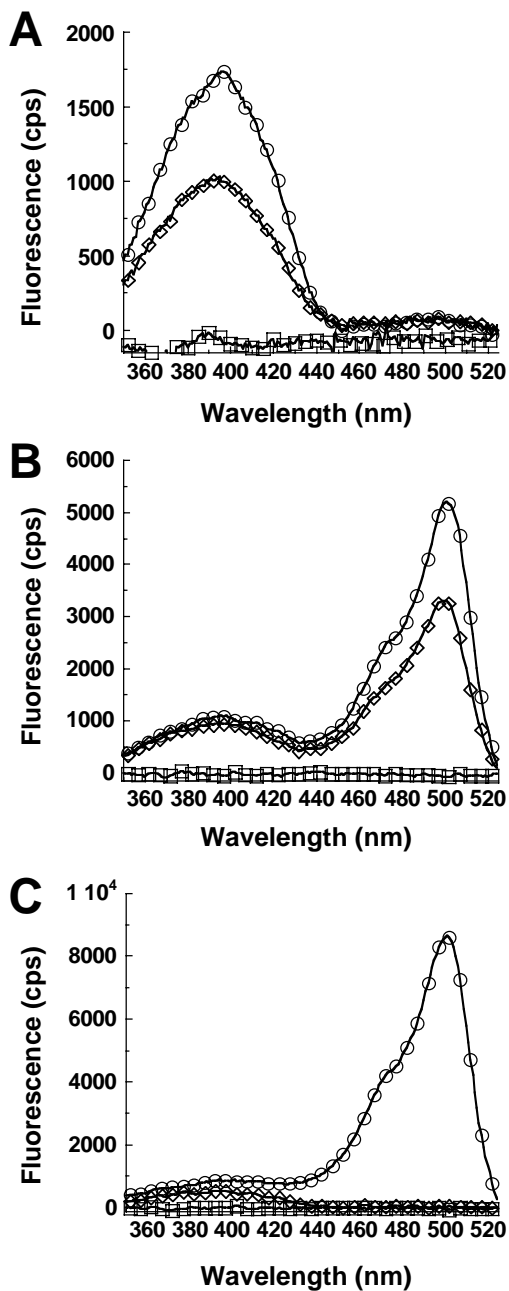
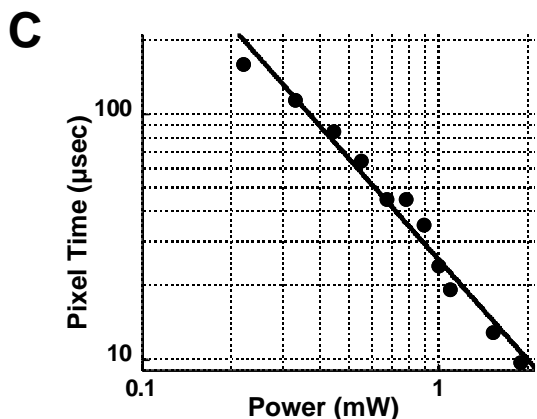
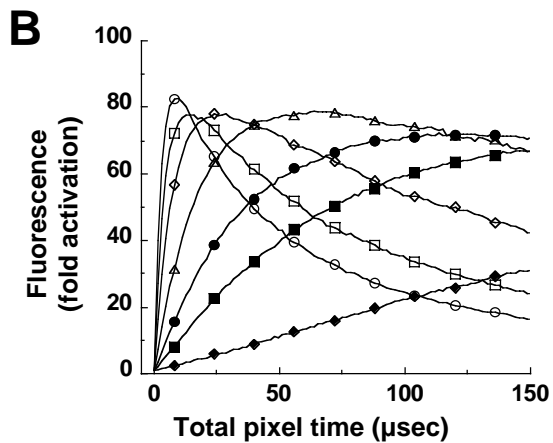
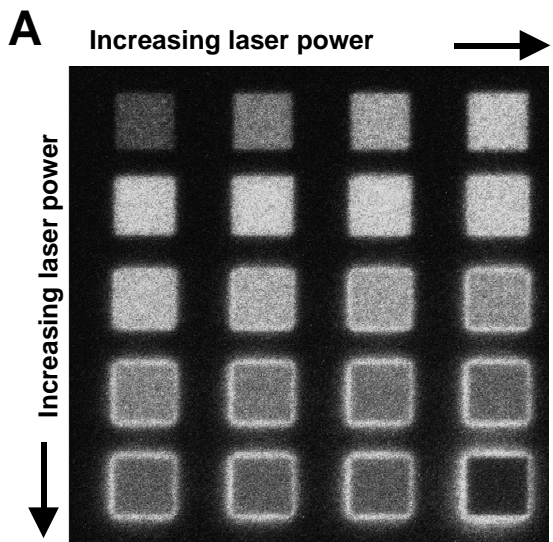


Figure 4. Excitation spectra of non-denatured, denatured, and refolded PA-GFP. Non-photoactivated PA-GFP (400 μ M) or photoactivated PA-GFP (400 μ M) was diluted to 4 μ M in PBS + 1 mM DTT and again diluted to 40 nM in PBS + 1 mM DTT to produce non-denatured PA-GFP. Alternatively, to produce denatured PA-GFP, non-photoactivated PA-GFP (400 μ M) was diluted to 4 μ M in 8M urea + 1 mM DTT and incubated at 95 $^{\circ}$ C for 5 minutes. The sample was then diluted to 40 nM in 8M urea + 1 mM DTT to maintain the denatured state or diluted to 40 nM in PBS + 1 mM DTT to refold PA-GFP. (A) Excitation spectra (350 nm-525 nm) were acquired by collecting the fluorescence emission at 550 nm with 25 nm slit widths of non-photoactivated PA-GFP in the non-denatured (open circles), denatured (open squares), and refolded (open diamonds) states. All spectra are background subtracted. (B) Excitation spectra (350 nm-525 nm) were acquired by collecting the fluorescence emission at 550 nm with 25 nm slit widths of photoactivated PA-GFP in the non-denatured (open circles), denatured (open squares), and refolded (open diamonds) states. All spectra are background subtracted. (C) Non-photoactivated PA-GFP (400 μ M) was maintained in a non-denatured state by dilution to 4 μ M in PBS + 1 mM DTT or it was denatured by dilution to 4 μ M in 8M urea + 1 mM DTT and incubated at 95 $^{\circ}$ C for 5 minutes. Each sample was irradiated with 25 mW of 413 nm laser light for 30 minutes at room temperature. The non-denatured sample was further diluted to 40 nM in diluted to 40 nM in PBS + 1 mM DTT to maintain the non-denatured protein (open circles). The denatured sample was diluted in 8M urea + 1 mM DTT to maintain the denatured state (open squares) or diluted to 40 nM in PBS + 1 mM DTT to refold PA-GFP (open diamonds). Excitation spectra (350 nm-525 nm) were acquired by collecting the fluorescence emission at 550 nm with 25 nm slit widths. All spectra are background subtracted.

3.3 Photoactivation mechanism

Although we are far from understanding the mechanism for PA-GFP photoactivation, these data suggest that it differs markedly from the original model for wild type GFP photoconversion. As mentioned earlier, the anionic chromophore (photoactivated) is thought to be stabilized by the hydroxyl group of the wild type T203^{28,29}. However, substitution of the threonine with many different residues which lack a hydroxyl group still develop proteins that can produce stable photoactivated absorbance spectra (Fig. 2), which may represent a shift in the chromophore population toward the anionic form. This suggests that the stabilization may occur by interactions with residue(s) other than or in addition to T203. Furthermore, the reacquisition of its previous pre-activated or post-activated form after denaturation and refolding suggests a covalent modification of the chromophore or surrounding residues. One possibility is the decarboxylation of E222, reported to occur in wild type GFP upon irradiation³¹. The loss of this moiety in such close proximity to the chromophore is expected to have dramatic effects on the ionic state of the chromophore and may be sufficient for formation of the anionic chromophore. If this is occurring in PA-GFP upon photoactivation, it would explain the remarkable stability of the post-activated form (Fig. 3 and 4B).



3.4 Using Photoactivatable GFP

Just as with photobleaching of other fluorophores, photoactivation of PA-GFP is dependent on the duration of excitation power per unit area. We can most easily demonstrate power dependence qualitatively using embedded purified PA-GFP. Excitation of the embedded PA-GFP with 488 nm laser light produces little fluorescence until irradiation of the square regions in figure 5A with different powers of 413 nm laser light. Generally, as the 413 nm power level increases, the level of photoactivation increases. However, PA-GFP photoactivation and photobleaching appear to be competing processes. At the lower power levels in figure 5A, photoactivation dominates and a fluorescence signal with good contrast over background is produced. However, at higher excitation powers, photobleaching dominates and a signal with less contrast compared with background is obtained.

3.4 Using Photoactivatable GFP

Just as with photobleaching of other fluorophores, photoactivation of PA-GFP is dependent on the duration of excitation power per unit area. We can most easily demonstrate power dependence qualitatively using embedded purified PA-GFP. Excitation of the embedded PA-GFP with 488 nm laser light produces little fluorescence until irradiation of the square regions in figure 5A with different powers of 413 nm laser light. Generally, as the 413 nm power level increases, the level of photoactivation increases. However, PA-GFP photoactivation and photobleaching appear to be competing processes. At the lower power levels in figure 5A, photoactivation dominates and a fluorescence signal with good contrast over background is produced. However, at higher excitation powers, photobleaching dominates and a signal with less contrast compared with background is obtained.

Figure 5. Photoactivation of PA-GFP under imaging conditions. (A) Purified PA-GFP was embedded in polyacrylamide. Each of the small squares was briefly irradiated with increasing levels of 413 nm laser light as indicated and the entire field was imaged using 488 nm laser light. (B) Purified PA-GFP was embedded in polyacrylamide and alternately imaged using 488 nm light and photoactivated with different 413 nm laser levels. These power levels, 0.108 mW (closed diamonds), 0.22 mW (closed squares), 0.33 mW (closed circles), 0.55 mW (open triangles), 1.0 mW (open diamonds), 1.54 mW (open squares), and 2.1 mW (open circles), were measured at the rear aperture of the objective. The pixel time was held constant at 1.6 µsec and the fold increase in fluorescence is displayed as the total photoactivation time per pixel. (C) Each data point represents the pixel time required to reach apex of one of the photoactivation curves as performed in figure 5B. The solid line represents a linear fit of a log-log plot (not shown) of the laser power and the total pixel time.

A hint at the effects of duration of irradiation is shown for wild type GFP in figure 1 and is further demonstrated for PA-GFP in figure 5B. These data represent quantification of fluorescence from embedded PA-GFP alternately imaged with 488 nm light and photoactivated with different powers of 413 nm light. The pixel dwell time (irradiation time per pixel) during photoactivation was held constant and is displayed as the total photoactivation time per pixel. The level of fluorescence increases exponentially to an apex and then decreases over longer exposure times. This decrease due to photobleaching is most evident at the higher laser powers and longer irradiation times. The apex of the curves in figure 5B represent the highest fold activation in fluorescence, so this point is defined as the total pixel time required for optimal photoactivation in an imaging experiment. The relationship between the total pixel time and 413 nm power level required for optimal photoactivation is shown in the log-log plots (Fig. 5C).

Photoactivation of PA-GFP expressed in living COS 7 cells was tested by imaging the cells prior to and after irradiation with the optimal amount of 413 nm laser light²³. For comparison, we imaged cells expressing WEGFP and found significant fluorescence at 488 nm excitation before photoactivation. This fluorescence was distributed uniformly throughout the cell and upon photoactivation, an increase of ~2.6-fold was measured. Alternatively, cells expressing PA-GFP displayed virtually no fluorescence at 488 nm excitation before photoactivation and increased ~62-fold after photoactivation.

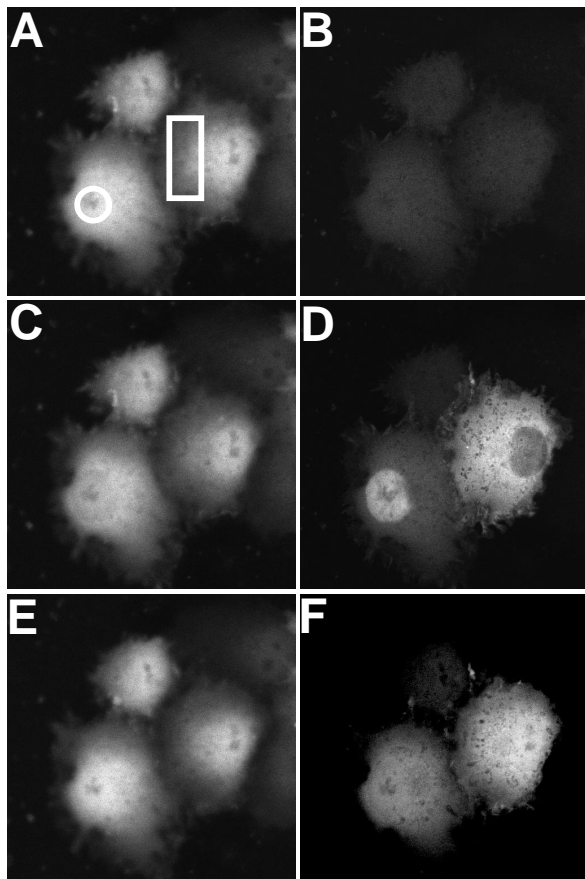


Figure 6. PA-GFP was expressed in COS 7 cells and imaged under excitation with low levels of 413 nm laser light (A, C, E) and with low levels of 488 nm laser light (B, D, F). Images were acquired prior to photoactivation (A, B) and after photoactivation (C-F) of the regions indicated by the circle and rectangle in figure A. The images immediately (C, D) and 13 minutes (E, F) after photoactivation show increased fluorescence under 488 nm excitation (D, F).

Figure 6 demonstrates a simple, yet compelling, test and demonstration of PA-GFP photoactivation in living cells. The left images (Fig. 6A, C, E) represent the fluorescence of free PA-GFP expressed in a COS 7 cell when imaged using low levels of 413 nm excitation and the green images (Fig. 6B, D, F) represent the fluorescence when imaged using 488 nm excitation. Prior to photoactivation, PA-GFP was observed throughout the cytoplasm and nucleus under low-level 413 nm illumination with little fluorescence observed under 488 nm excitation. After photoactivation within the regions denoted by the circle in one cell and the rectangle in a second cell (Fig. 6A), nuclear (cell on the left) or cytoplasmic (cell on the right) fluorescence signals, respectively, were observed at the initial post-photoactivation time point when imaged with 488 nm excitation. Because GFP has a cytoplasmic diffusion coefficient of $2\text{-}3\text{ cm}^2\text{ sec}^{-1}$ ³⁵, the photoactivated protein rapidly diffused throughout the nucleus or cytoplasm but was slowed by the nuclear envelope, which acts as a diffusion barrier (Fig. 6D). However, as expected for a GFP molecule without a specific cellular targeting sequence, the photoactivated nuclear and cytoplasmic pools of PA-GFP equilibrated with their complementary non-photoactivated compartment presumably by diffusion through the nuclear pores (Fig. 6E-6F). Thus, by photoactivating selectively a pool of molecules, the movement of these molecules from the selected region and the movement into other regions could easily be monitored.

3. SUMMARY

We have described our development and testing of a photoactivatable variant of the *Aequorea victoria* GFP, PA-GFP²³. Upon photoactivation, PA-GFP exhibits an optical enhancement of nearly two orders of magnitude under aerobic conditions. We anticipate that photoactivation of PA-GFP and other photoactivatable fluorescent proteins

^{20,22} will nicely complement existing photobleaching techniques techniques, such as fluorescence recovery after photobleaching (FRAP) and fluorescence loss in photobleaching (FLIP)⁸⁻¹⁴, for monitoring intracellular protein dynamics. Unlike most photobleaching techniques, photoactivation allows the investigator to selectively and directly highlight protein populations within cells or cells within a population. This characteristic of PA-GFP photoactivation offers some subtle advantages in live cell imaging. For instance, we found that photoactivation could generate fluorescent molecules much more rapidly and with greater optical enhancement than photobleaching could generate non-fluorescent EGFP molecules for use in protein tracer experiments. A more powerful laser could help to reduce the photobleaching time in such experiments, but it would not change the inherent photostability of EGFP (i.e., resistance to photobleaching). A more important advantage is that only photoactivated PA-GFP molecules exhibit marked fluorescence. Because of this, there is no concern that newly synthesized molecules will become fluorescent and complicate the results as can occur in photobleaching studies aimed at measuring protein dynamics⁸. Our rationale for this is that a molecule that has not been synthesized certainly cannot be photoactivated and figure 4C argues that a protein molecule that is not properly folded cannot be photoactivated. Thus, by acting as an "optical pulse label", PA-GFP provides a powerful new tool for monitoring protein trafficking, protein turnover, cell lineage, and cell migration and will assist in investigating fundamental cell and developmental biology questions^{13,14}.

ACKNOWLEDGEMENTS

G.P. was an Intramural Research Training Award fellow during this work.

REFERENCES

1. Politz, J. C., "Use of caged fluorophores to track macromolecular movement in living cells", *Trends in Cell Biology*, **9**, 284-287, 1999.
2. Chalfie, M., Tu, Y., Euskirchen, G., Ward, W. W. & Prasher, D. C., "Green fluorescent protein as a marker for gene expression", *Science*, **263**, 802-805, 1994.
3. Tsien, R. Y., "The green fluorescent protein", *Annual Review of Biochemistry*, **67**, 509-544, 1998.
4. Ward, W. W., in *Bioluminescence and Chemiluminescence* (eds. DeLuca, M. A. & McElroy, W. D.) 235-242 (Academic Press, Inc., New York, 1981).
5. Bokman, S. & Ward, W. W., "Renaturation of *Aequorea* green fluorescent protein", *Biochemical and Biophysical Research Communications*, **101**, 1372-1380, 1981.
6. Ward, W. W. & Bokman, S. H., "Reversible denaturation of *Aequorea* green-fluorescent protein: physical separation and characterization of the renatured protein", *Biochemistry*, **21**, 4535-4540, 1982.
7. Ward, W. W., Prentice, H. J., Roth, A. F., Cody, C. W. & Reeves, S. C., "Spectral perturbations of the *Aequorea* green-fluorescent protein", *Photochemistry and Photobiology*, **35**, 803-808, 1982.
8. Lippincott-Schwartz, J., Snapp, E. & Kenworthy, A., "Studying protein dynamics in living cells", *Nature Reviews Molecular Cell Biology*, **2**, 444-456, 2001.
9. Houtsmuller, A. B. & Vermeulen, W., "Macromolecular dynamics in living cell nuclei revealed by fluorescence redistribution after photobleaching", *Histochemistry and Cell Biology*, **115**, 13-21, 2001.
10. Phair, R. D. & Misteli, T., "Kinetic modeling approaches to in vivo imaging", *Nature Reviews Molecular Cell Biology*, **2**, 898-907, 2001.
11. Klonis, N. et al., "Fluorescence photobleaching analysis for the study of cellular dynamics", *Eur Biophys J*, **31**, 36-51, 2002.
12. van Roessel, P. & Brand, A. H., "Imaging into the future: visualizing gene expression and protein interactions with fluorescent proteins", *Nature Cell Biology*, **4**, E15-E20, 2002.
13. Lippincott-Schwartz, J. & Patterson, G. H., "Development and use of fluorescent protein markers in living cells", *Science*, **300**, 87-91, 2003.
14. Lippincott-Schwartz, J., Altan-Bonnet, N. & Patterson, G. H., "Photobleaching and photoactivation: following protein dynamics in living cells", *Nature Cell Biology*, **5**, S7-S14, 2003.
15. Chatteraj, M., King, B. A., Bublitz, G. U. & Boxer, S. G., "Ultra-fast excited state dynamics in green fluorescent protein: Multiple states and proton transfer", *Proc. Natl. Acad. Sci. USA*, **93**, 8362-8367, 1996.
16. Yokoe, H. & Meyer, T., "Spatial dynamics of GFP-tagged proteins investigated by local fluorescence enhancement", *Nature Biotechnology*, **14**, 1252-1256, 1996.

17. Elowitz, M. B., Surette, M. G., Wolf, P.-E., Stock, J. & Leibler, S., "Photoactivation turns green fluorescent protein red", *Current Biology*, **7**, 809-812, 1997.
18. Sawin, K. E. & Nurse, P., "Photoactivation of green fluorescent protein", *Current Biology*, **7**, R606-R607, 1997.
19. Lukyanov, K. A. et al., "Natural animal coloration can be determined by a nonfluorescent green fluorescent protein homolog", *The Journal of Biological Chemistry*, **275**, 25879-25882, 2000.
20. Chudakov, D. M. et al., "Kindling fluorescent proteins for precise *in vivo* photolabeling", *Nature Biotechnology*, **21**, 191-194, 2003.
21. Marchant, J. S., Stutzmann, G. E., Leissring, M. A., LaFerla, F. M. & Parker, I., "Multiphoton-evoked color change of DsRed as an optical highlighter for cellular and subcellular labeling", *Nature Biotechnology*, **19**, 645-649, 2001.
22. Ando, R., Hama, H., Yamamoto-Hino, M., Mizuno, H. & Miyawaki, A., "An optical marker based on the UV-induced green-to-red photoconversion of a fluorescent protein", *Proceedings of the National Academy of Science, USA*, **99**, 12651-12656, 2002.
23. Patterson, G. H. & Lippincott-Schwartz, J., "A photoactivatable GFP for selectively photolabeling of proteins and cells", *Science*, **297**, 1873-1877, 2002.
24. Patterson, G. H., Knobel, S. M., Sharif, W. D., Kain, S. R. & Piston, D. W., "Use of the green-fluorescent protein (GFP) and its mutants in quantitative fluorescence microscopy", *Biophysical Journal*, **73**, 2782-2790, 1997.
25. Ormö, M. et al., "Crystal structure of the *Aequorea victoria* green fluorescent protein", *Science*, **273**, 1392-1395, 1996.
26. Yang, F., Moss, L. G. & Phillips, G. N., Jr., "The molecular structure of the green fluorescent protein", *Nature Biotechnology*, **14**, 1246-1251, 1996.
27. Cody, C. W., Prasher, D. C., Westler, W. M., Prendergast, F. G. & Ward, W. W., "Chemical structure of the hexapeptide chromophore of the *Aequorea* green-fluorescent protein", *Biochemistry*, **32**, 1212-1218, 1993.
28. Brejc, K. et al., "Structural basis for the dual excitation and photoisomerization of the *Aequorea victoria* green fluorescent protein", *Proceedings of the National Academy of Science USA*, **94**, 2306-2311, 1997.
29. Palm, G. J. et al., "The structural basis for spectral variations in green fluorescent protein", *Nature Structural Biology*, **4**, 361-365, 1997.
30. Creemers, T. M. H., Lock, A. J., Subramaniam, V., Jovin, T. M. & Völker, S., "Three photoconvertible forms of green fluorescent protein identified by spectral hole-burning", *Nature Structural Biology*, **6**, 557-560, 1999.
31. van Thor, J. J., Gensch, T., Hellingwerf, K. J. & Johnson, L. N., "Phototransformation of green fluorescent protein with UV and visible light leads to decarboxylation of glutamate 222", *Nature Structural Biology*, **9**, 37-41, 2002.
32. Heim, R., Prasher, D. C. & Tsien, R. Y., "Wavelength mutations and posttranslational autooxidation of green fluorescent protein", *Proc. Natl. Acad. Sci. USA*, **91**, 12501-12504, 1994.
33. Ehrig, T., O'Kane, D. J. & Prendergast, F. G., "Green-fluorescent protein mutants with altered fluorescence excitation spectra", *FEBS Letters*, **367**, 163-166, 1995.
34. Kummer, A. D. et al., "Effects of threonine 203 replacements on excited-state dynamics and fluorescence properties of the green fluorescent protein (GFP)", *Journal of Physical Chemistry B*, **104**, 4791-4798, 2000.
35. Verkman, A. S., "Solute and macromolecule diffusion in cellular aqueous compartments", *Trends in Biochemical Sciences*, **2**, 27-33, 2002.